

Transport calculation of semiconductor nanowires coupled to quantum well reservoirs

Mathieu Luisier · Andreas Schenk ·
Wolfgang Fichtner · Gerhard Klimeck

Published online: 9 December 2006
© Springer Science + Business Media, LLC 2007

Abstract Semiconductor nanowires are possible candidates to replace the metal-oxide-semiconductor field-effect transistors (MOSFET) since they can act both as active devices or as device connectors. In this article, the transmission coefficients of Si and GaAs nanowires with arbitrary transport directions and cross sections are simulated in the nearest-neighbor $sp^3d^5s^*$ semi-empirical tight-binding method. The open boundary conditions (OBC) are calculated with a new scattering boundary method where a normal eigenvalue problem of reduced size is solved. Two different types of contacts are studied. In the ideal case, semi-infinite reservoirs (the source and the drain) that are the prolongation of the device are assumed. In a more realistic configuration, the active nanowire is embedded between two quantum well (QW) reservoirs. The electrical properties of the device are obtained by a non-equilibrium Green's function (NEGF) calculation.

Keywords Nanowires · Tight-binding method · NEGF · Open boundary conditions

1 Introduction

Recently, nanoscale field-effect transistors (FET) have been realized with an individual nanowire (NW) and reported in the literature [1]. To properly describe and model the ballistic current flow in such devices, classical concepts should be

abandoned. It is necessary to include quantum transport phenomena such as the two-dimensional confinement of the electrons (or holes) in the channel. In a first approximation, this effect strongly depends on the choice of the effective masses used in the directions of confinement. A more accurate treatment consists in taking the full bandstructure into account and not only points of high symmetry in the Brillouin Zone (BZ). In this work, therefore, an atomistic treatment of Si and GaAs nanowires based on the nearest-neighbor $sp^3d^5s^*$ semi-empirical tight-binding method is chosen.

As the metallic contacts (Ti for example) of such devices are often much wider than the device itself, they are modeled as quantum well (QW) reservoirs with charge confinement in one direction only. As a first approximation, the contacts are made of the same semiconducting material as the nanowire. The resulting transmission coefficients are compared to the ideal case, where the contacts are semi-infinite prolongation of the device. The open boundary conditions (OBC) are calculated for both applications with a new scattering boundary method [2] that is summarized in the next Section. Results are shown in Section 3 for Si and GaAs nanowires whose transport direction is arbitrarily chosen. A conclusion is given in Section 4.

2 Theory

In this Section, the computational procedure to obtain open boundary conditions in two-dimensionally confined nanowires with perfect and with more realistic QW contacts is outlined, followed by its coupling to a NEGF solver. The perfect contacts case was already described in [2] and can be generalized to other contact types such as QW. More algebraic details will be published elsewhere.

M. Luisier (✉) · A. Schenk · W. Fichtner
Integrated Systems Laboratory, Gloriastrasse 35 ETH Zurich,
8092 Zurich, Switzerland
e-mail: mluisier@iis.ee.ethz.ch

G. Klimeck
Network for Computational Nanotechnology, Purdue University,
West Lafayette, IN 47907, USA

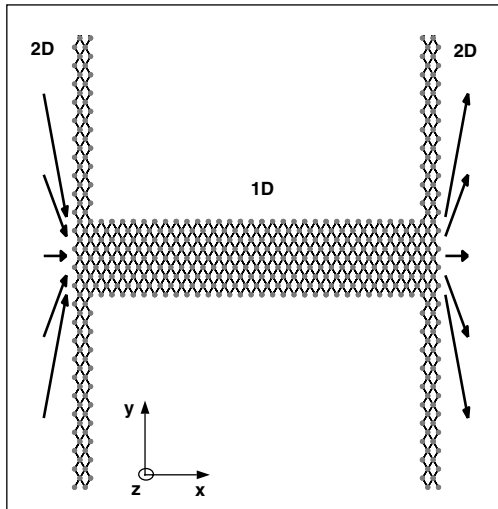


Fig. 1 Schematic top view of a Si nanowire embedded between two quantum well reservoirs. x is the transport direction ([100]), y has confinement in the nanowire and is open in the quantum wells ([010]), and z is a direction of confinement everywhere ([001]). Injection in the nanowire occurs from all the allowed (k_x, k_y) combinations at a given energy E

A top view of a Si nanowire ($x = [100]$, $y = [010]$, and $z = [001]$) embedded between two QW reservoirs (same crystal orientations as the wire) is depicted in Fig. 1. Although strain, surface reconfiguration, and surface passivation could play an important role for wires of such large surface-to-volume ratio, they are not considered in this study. In the nanowire (labeled 1D), the electrons are free only in their transport direction x , but are confined in the y and z directions. In the two QW reservoirs (labeled 2D), the electrons can freely move along x and y , but are confined in z direction. Consequently, transitions between a one-dimensionally confined electron gas (1DEG) and a 2DEG exist at the QW-wire interfaces.

In any scattering boundary method [2–4] with ideal contacts, at a given energy E , states $\phi_n(E)$ are injected from the reservoirs into the device for all the authorized wave vectors $k_x(E)$ aligned with the wire transport direction x . QW reservoirs add a third variable k_y related to possible displacements in the y direction for the 2DEG. Instead of depending on the injection energy E only, the reservoir states $\phi_n(E, k_y)$ and wave vectors $k_x(E, k_y)$ are also calculated for all the possible k_y in the first two-dimensional QW Brillouin Zone. In Fig. 1, different injection directions are shown on the left and possible output trajectories on the right.

Figure 2 describes how to compute the $k_x(E, k_y)$ and $\phi_n(E, k_y)$ in the QW reservoirs. First, the QW unit cell must be determined. For a wire with the same crystal orientations as in Fig. 1, its primitive unit cell (projected onto the (x, y) plane) is shown in the upper part of Fig. 2. By translating it with the vectors v_1 and v_2 , the semi-infinite QW reservoirs

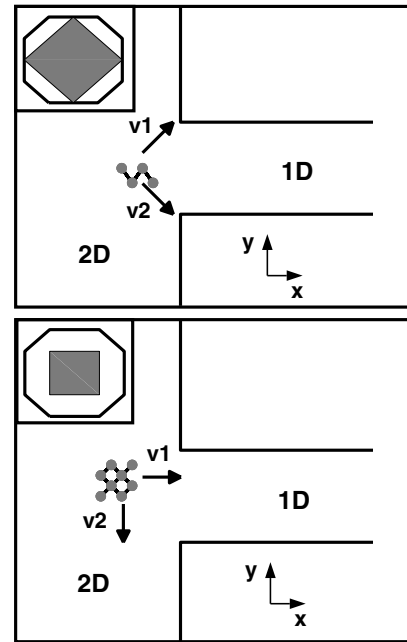


Fig. 2 Projection of the quantum well unit cell onto the (x, y) plane with the displacement vectors v_1 and v_2 . The growth direction z is aligned with [001] and the transport direction in the wire x with [100]. Top: primitive QW unit cell. The projection contains four atoms (gray dots). Bottom: new QW unit cell with v_1 and v_2 aligned with x and y (projection contains eight atoms). Both insets show the corresponding two-dimensional Brillouin Zone drawn in a cut plane of the three-dimensional one at $k_z = 0$

can be totally spanned. Although this unit cell is the smallest one, it is not well suited to be coupled to a nanowire. Since the device transport direction is x , it is advantageous to have v_1 or v_2 aligned with it and the other vector aligned with y . For that purpose, a larger unit cell fulfilling this condition is constructed in the lower part of Fig. 2. Note that the size of the corresponding two-dimensional BZ is divided by two and the QW bandstructure is folded.

For the nanowire in Fig. 1, the $\phi_n(E, k_y)$'s are the eigenstates of the unit cell shown in the lower part of Fig. 2 and comprising $8 \times N_{LC}$ atoms. N_{LC} is the number of lattice constants a_0 composing the QW width L_z in the z direction. For instance, if $L_z = 3a_0$ then $N_{LC} = 3$. The $\phi_n(E, k_y)$'s are vectors of size $N = 8 \times N_{LC} \times t_b$, where t_b is the number of atomic orbitals taken into account. In the $sp^3d^5s^*$ tight-binding method, $t_b = 10$ without spin-orbit (SO) coupling and $t_b = 20$ with SO.

$k_x(E, k_y)$ and $\phi_n(E, k_y)$ can be obtained from the solution of a generalized eigenvalue problem of size $2N$ [3, 4]. However, simplifications in the structure of the involved matrices lead to a more efficient algorithm based on a usual eigenvalue problem with size $\leq N$ [2]. This approach works for all the possible crystal orientations and not only for $x = [100]$ and $y = [010]$.

From $k_x(E, k_y)$ and $\phi_n(E, k_y)$, a reservoir Green's function $g^R(E)$ is evaluated and cast into a self-energy $\Sigma^R(E)$

[2, 3]. Finally, a recursive atomistic NEGF scheme [5] is applied to calculate the ballistic nanowire electrical properties, such as the transmission coefficient $T(E)$.

3 Results

Simulations of Si and GaAs nanowires with different cross sections and crystal orientations (see Fig. 3 for a (y, z) projection of the wire cross sections), but with almost the same wire length $L_w = 22.5 \pm 0.5$ nm are presented in this Section. The width of the QW reservoirs L_z corresponds to the maximal height of the nanowire embedded between them. Thus $L_z = 1.6$ nm for the Si rectangular wire ($x = [100]$, $y = [010]$), 1.2 nm for the Si triangular wire ($x = [111]$, $y = [\bar{1}10]$), 1.7 nm for the Si circular wire ($x = [100]$, $y = [011]$), and 1.2 nm for the GaAs rectangular wire ($x = [113]$, $y = [\bar{1}10]$). In fact, as long as L_z is equal or larger to the maximal height of the nanowire cross section, there is no restriction for its choice. However, the more atoms the QW unit cell has, the more expensive the computational effort to obtain $\phi_n(E, k_y)$ becomes.

The $sp^3d^5s^*$ tight-binding parameters were optimized by T.B. Boykin et al. to reproduce Si [6] and GaAs [7] bulk bandstructures. They are assumed unchanged for the QW and nanowire structures simulated in this work. Spin-orbit coupling is neglected because electron transmission is considered and its effects are small on the conduction band [2].

Figure 4 shows the transmission coefficients $T(E)$ for the four unbiased nanowires in Fig. 3. $E = 0$ eV is the top of the bulk valence band. For each different cross section, two curves are calculated. The bright lines illustrate the ideal case, i.e. the semi-infinite source and drain are the prolongation of the nanowire. Since the reservoirs and the central device they are connected to form a uniform infinite nanowire, each step in $T(E)$ corresponds to the turn-on of a new band in the NW bandstructure [8].

The dark lines in Fig. 4 result from the transmission calculation in nanowires with two quantum well reservoirs. These curves exhibit strong interference effects caused by the 2DEG-1DEG transitions. Thus the nanowires behave like a resonant cavity delimited by two large areas, the source and the drain. The ideal case forms a kind of upper limit that cannot be exceeded. For the Si rectangular wire (x aligned with [100], subplot(a)), the transmission calculated with QW reservoirs converges towards the bright line. If a plateau is large enough, the $T(E)$ oscillations become smaller and smaller and their peaks closer to the upper limit.

Although the trends given by the bright lines are also followed by the nanowires (b), (c), and (d), one sees that the differences are bigger and the oscillation amplitudes larger, especially for the rectangular GaAs device with an exotic transport direction $x = [113]$. The rapid changes in the ideal

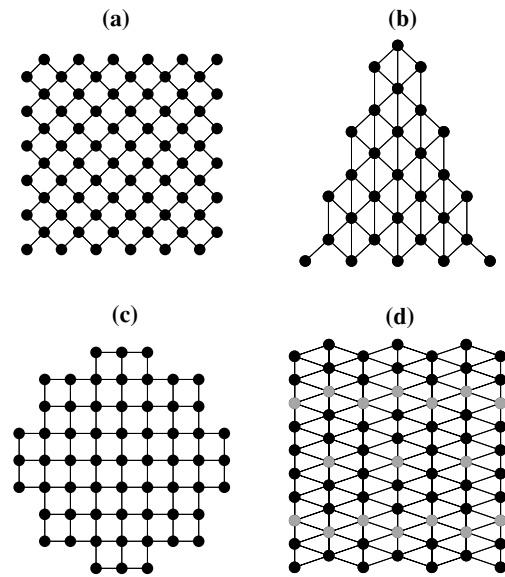


Fig. 3 Projection onto the (y, z) plane of the cross section of the different nanowires simulated in this work: (a) Si rectangular wire (1.6 nm \times 1.6 nm, transport $x = [100]$, $y = [010]$), (b) Si triangular wire (base = 1.6 nm, height = 1.2 nm, transport $x = [111]$, $y = [\bar{1}10]$), (c) Si circular wire (radius $r = 0.85$ nm, transport $x = [100]$, $y = [011]$), and (d) GaAs rectangular wire (1.2 nm \times 1.2 nm, transport $x = [113]$, $y = [\bar{1}10]$, Ga atoms are dark, As atoms are bright)

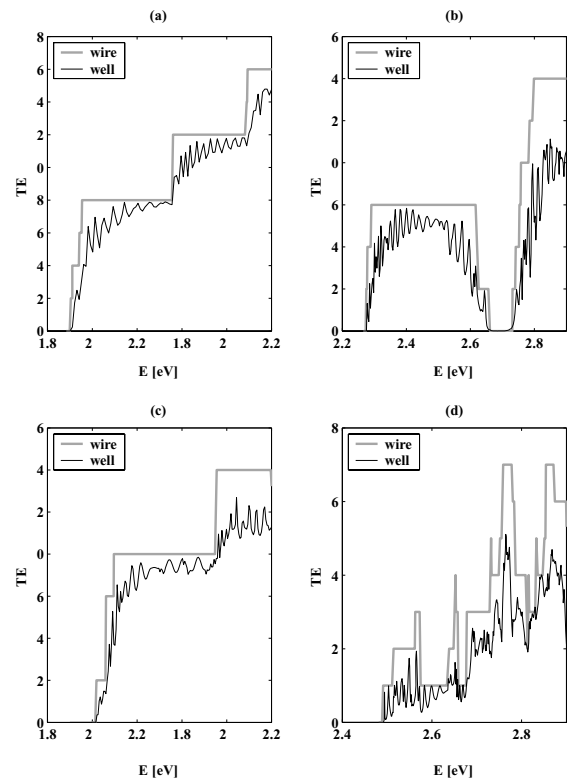


Fig. 4 Electron transmission through the nanowires described in Fig. 3 calculated without spin-orbit coupling. The bright lines correspond to nanowires with two perfect wire contacts, the dark lines to nanowires embedded between two QW reservoirs

$T(E)$, characterized by the multiple appearance and disappearance of subbands in the nanowire device, can only be reproduced with difficulty when QW reservoirs are inserted.

4 Conclusion

In this work, the transmission coefficient of Si and GaAs nanowires with different crystal orientations, cross sections, and contact types (perfect or quantum well) has been simulated in the $sp^3d^5s^*$ semi-empirical tight-binding method. The open boundary conditions are treated with a new efficient method and are then coupled to a NEGF solver. As a next step, strain and surface reconfiguration should be included in a self-consistent treatment (transport and electrostatics) of nanowires with ideal or quantum well reservoirs.

Acknowledgments M.L. is supported by the Swiss National Fond (SNF), project 200021-109393 (NEQUATTRO). G.K. is supported by the National Science Foundation under Grant No. EEC-0228390.

References

1. Cui, Y., Zhong, Z., Wang, D., Wang, W.U., Lieber, C.: High performance silicon nanowire. *Nano Lett.* **3**, 149 (2003)
2. Luisier, M., Schenk, A., Fichtner, W., Klimeck, G., Atomistic simulation of nanowires in the $sp^3d^5s^*$ tight-binding formalism: from boundary conditions to strain calculations. In press *Phys. Rev. B* (2006)
3. Rivas, C., Lake, R.: Non-equilibrium Green function implementation of boundary conditions for full band simulations of substrate-nanowire structures. *Phys. Stat. Sol. (b)* **239**, 94 (2003)
4. Stadele, M., Tuttle, B.R., Hess, K.: Tunneling through ultrathin SiO_2 gate oxides from microscopic models. *J. Appl. Phys.* **89**, 348 (2001)
5. Lake, R., Klimeck, G., Bowen, R.C., Jovanovic, D.: Single and multi-band modeling of quantum electron transport through layered semiconductor devices. *J. Appl. Phys.* **81**, 7845 (1997)
6. Boykin, T.B., Klimeck, G., Oyafuso, F.: Valence band effective-mass expression in the $sp^3d^5s^*$ empirical tight-binding model applied to a Si and Ge parametrization. *Phys. Rev. B* **69**, 115201 (2004)
7. Boykin, T.B., Klimeck, G., Bowen, R.C., Oyafuso, F.: Diagonal parameter shifts due to nearest-neighbor displacements in empirical tight-binding theory. *Phys. Rev. B* **66**, 125207 (2002)
8. Ko, Y.-J., Shin, M., Lee, S., Park, K.W.: Effects of atomistic defects on coherent electron transmission in Si nanowires: Full band calculations. *J. Appl. Phys.* **89**, 374 (2001)